A Cohesive Lagrangian Swarm and Its Application to Multiple Unicycle-like Vehicles

Jito Vanualailai and Bibhya Sharma

Abstract—Swarm principles are increasingly being used to design controllers for the coordination of multi-robot systems or, in general, multi-agent systems. This paper proposes a two-dimensional Lagrangian swarm model that enables the planar agents, modeled as point masses, to swarm whilst effectively avoiding each other and obstacles in the environment. A novel method, based on an extended Lyapunov approach, is used to construct the model. Importantly, the Lyapunov method ensures a form of practical stability that guarantees an emergent behavior, namely, a cohesive and well-spaced swarm with a constant arrangement of individuals about the swarm centroid. Computer simulations illustrate this basic feature of collective behavior. As an application, we show how multiple planar mobile unicycle-like robots swarm to eventually form patterns in which their velocities and orientations stabilize.

Keywords—Attractive-repulsive swarm model; individual-based swarm model; Lagrangian swarm model; Lyapunov stability; Lyapunov-like function; practical stability; unicycle.

I. INTRODUCTION

THE collective motion of organisms, as exhibited, for example, by schools of fish, flocks of birds, herds of mammals and swarms of bacteria, has, for many years, fascinated scientists, who yearned to understand the underlying cooperative dynamics [1]. The fact that certain engineering problems in Artificial Intelligence can be solved in an ingenious way by roughly mimicking this natural phenomenon [2], [3] has led to greater efforts by mathematicians, engineers, computer scientists, physicists and biologists, in recent years, to seek better understanding of self-organization in organisms, and the formation and the persistence of aggregation [4], [5]. From their work, it is now possible to categorize the approaches for developing a model of a biological swarm into two: the *Eulerian* and the *Lagrangian* approaches [1], [4], [6]–[9]. In the Eulerian approach, the swarm is considered a *continuum* described by its density in one-, two- or three-dimensional space. The time evolution of animal density is usually modeled by partial differential equations. In the Lagrangian approach, the state (position, instantaneous velocity and instantaneous acceleration) of each individual and its relationship with other individuals in the swarm is studied; it is an *individual-based* approach, in which the velocity and acceleration can be influenced by spatial coordinates of the individual. The time evolution of the state is usually described by ordinary or stochastic differential equations. Comprehensive reviews of these approaches and their advantages and disadvantages can also be found in [10] and [11].

Lagrangian swarm models, with attractive-repulsive inter-individual interaction, assume that swarming behavior is a result of the interplay between a long-range attraction and a short-range repulsion between the individuals in the swarm, with the centroid being the center of attraction [10], [12]. The pioneering paper by Gazi and Passino [12] went further by developing a Lagrangian model based on the Direct Method of Lyapunov and showing that the model is stable and exhibits an emergent behavior wherein there is a constant arrangement about the centroid. This paper shows, for the first time, that the concept of *practical stability* founded on an extended method of Lyapunov is also particularly effective in the construction of another Lagrangian swarm model due to the fact that biological swarming is a bounded activity about a central point, with no inter-individual collision. In such models, the centroid may not be stationary or may not be mathematically stable, yet the collective behavior of the individuals in the vicinity of the centroid is an emergent bounded pattern; that is, the model is practically stable. Via a Lyapunov-like function, we create the new and relatively simple individual-based continuous time model for swarm aggregation in two-dimensional space. The Lyapunov-like function, which has inter-individual attractive and collision-avoidance components, guarantees the practical stability of the model, shows that an emergent collective behavior is a constant arrangement about the centroid, and provides an approximation of the size and density of the swarm. Four parameters, which we call the *cohesion parameters*, *coupling parameters*, *obstacle avoidance parameters*, and *convergence parameters*, are utilized in the model. They are a measure of the strengths of the cohesion of the swarm, the interaction between any two individuals, the interaction between an individual and an obstacle, and the rate of convergence of an individual to the swarm centroid. By varying these parameters computer simulations illustrate basic features of collective behavior such as congregation of individuals about their centroid and avoidance due to the presence of fixed obstacles. Note the only known work on practical stability of swarm models are by Chen et al. in 2006 [13], Pan et al. in 2008 [14], [15] and Xue and Zeng in 2009 [16]. However, the models are the original Gazi-Passino swarm model and its variations [10], [12], which have already been shown to be Lyapunov stable. Moreover, the authors did not provide the biological motivations behind the necessity to apply the concept of practical stability.

The authors are with the School of Computing, Information & Mathematical Sciences, University of the South Pacific, Suva, Fiji.

Corresponding author: email: jito.vanualailai@usp.ac.fj, phone: +679 323 2661; fax: +679 323 1504

II. A Two-Dimensional Swarm Model and its Practical Stability

We shall construct a model of a swarm with n individuals moving with the velocity of the swarm's centroid. Following previous work such as those of [9] and [10], we consider the individuals as point masses. For clarity of exposition, we confine ourselves to constructing the two-dimensional version of the model; it is a simple matter to extend it to three-dimensional.

At time $t \geq 0$, let $(x_i(t), y_i(t))$, $i = 1, 2, \ldots, n$, be the planar position of the ith individual, which we shall define as a point mass residing in a disk of radius $r_i > 0$,

$$B_i = \{(z_1, z_2) \in \mathbb{R}^2 : (z_1 - x_i)^2 + (z_2 - y_i)^2 \leq r_i^2\}. \quad (1)$$

The disk is described in [9] as a *bin*, and in [10] as a *private or safety area* of each individual. We shall use the former term, with *bin size* being the radius r_i of the disk.

Let us define the *centroid of the swarm* as

$$(x_c, y_c) = \left(\frac{1}{n} \sum_{k=1}^{n} x_k, \frac{1}{n} \sum_{k=1}^{n} y_k \right). \quad (2)$$

At time $t \geq 0$, let $(v_i(t), w_i(t)) := (x_i'(t), y_i'(t))$ be the instantaneous velocity of the ith point mass. Using the above notations, we have thus a system of first-order ODEs for the ith individual, assuming the initial condition at $t = t_0 \geq 0$:

$$\left. \begin{array}{rcl} x_i'(t) &=& v_i(t), \\ y_i'(t) &=& w_i(t), \\ x_{i0} &:=& x_i(t_0), \\ y_{i0} &:=& y_i(t_0). \end{array} \right\} \quad (3)$$

Suppressing t, we let $\mathbf{x}_i = (x_i, y_i,) \in \mathbb{R}^2$ and $\mathbf{x} = (\mathbf{x}_1, \ldots, \mathbf{x}_n) \in \mathbb{R}^{2n}$ be our state vectors. Also, let

$$\mathbf{x}_0 = \mathbf{x}(t_0) = \underbrace{(x_{10}, y_{10}, \ldots, x_{n0}, y_{n0})}_{2n \text{ terms}}.$$

If $\mathbf{g}_i(\mathbf{x}) := (v_i, w_i) \in \mathbf{R}^2$ and $\mathbf{G}(\mathbf{x}) := (\mathbf{g}_1(\mathbf{x}), \ldots, \mathbf{g}_n(\mathbf{x})) \in \mathbb{R}^{2n}$, then our swarm system of n individuals is

$$\dot{\mathbf{x}} = \mathbf{G}(\mathbf{x}), \quad \mathbf{x}_0 = \mathbf{x}(t_0). \quad (4)$$

Let $\mathbf{x}_i^* := (x_c, y_c)$ for $i = 1, 2, \ldots, n$, and

$$\mathbf{x}^* = (\mathbf{x}_1^*, \ldots, \mathbf{x}_n^*)$$
$$= \underbrace{\left(\frac{1}{n} \sum_{k=1}^{n} x_k, \frac{1}{n} \sum_{k=1}^{n} y_k, \cdots, \frac{1}{n} \sum_{k=1}^{n} x_k, \frac{1}{n} \sum_{k=1}^{n} y_k \right)}_{2n \text{ terms}}.$$

Then we have the Euclidean norm

$$\|\mathbf{x} - \mathbf{x}^*\|$$
$$= \sqrt{\left(x_1 - \frac{1}{n} \sum_{k=1}^{n} x_k \right)^2 + \cdots + \left(y_n - \frac{1}{n} \sum_{k=1}^{n} y_k \right)^2}.$$

If $\mathbf{G} \in C[\mathbb{R}^{2n}, \mathbb{R}^{2n}]$, then we can invoke the definition of the practical stability of system (4) as provided by [17], noting that we do not need the existence of an equilibrium point of the system. In the definition, $\mathbb{R}_+ := [0, \infty)$.

Definition 1: System (4) is said to be

(PS1) *practically stable* if given (λ, A) with $0 < \lambda < A$, we have $\|\mathbf{x}_0 - \mathbf{x}^*\| < \lambda$ implies that $\|\mathbf{x}(t) - \mathbf{x}^*\| < A$, $t \geq t_0$ for some $t_0 \in \mathbb{R}_+$;

(PS2) *uniformly practically stable* if *(PS1)* holds for every $t_0 \in \mathbb{R}_+$.

The following comparison principle for practical stability is also adapted from [17] for system (4), where

$$S(\rho) := \{\mathbf{x} \in \mathbb{R}^{2n} : \|\mathbf{x} - \mathbf{x}^*\| < \rho\},$$

$$K = \{a \in C[\mathbb{R}_+, \mathbb{R}_+] :$$
$$a(u) \text{ is strictly increasing in } u \text{ and}$$
$$a(u) \to \infty \text{ as } u \to \infty\},$$

and, for any Lyapunov-like function $V \in C[\mathbb{R}_+ \times \mathbb{R}^{2n}, \mathbb{R}_+]$,

$$D^+ V(t, \mathbf{x}) := \limsup_{h \to 0^+} \frac{V(t + h, \mathbf{x} + h\mathbf{G}(\mathbf{x})) - V(t, \mathbf{x})}{h},$$

for $(t, \mathbf{x}) \in \mathbb{R}_+ \times \mathbb{R}^{2n}$, noting that if $V \in C^1[\mathbb{R}_+ \times \mathbb{R}^{2n}, \mathbb{R}_+]$, then $D^+ V(t, \mathbf{x}) = V'(t, \mathbf{x})$, where $V'(t, \mathbf{x}) = V_t(t, \mathbf{x}) + V_x(t, \mathbf{x})\mathbf{G}(\mathbf{x})$.

Theorem 1: ([17]) *Assume that*

1) λ *and* A *are given such that* $0 < \lambda < A$;
2) $V \in C[\mathbb{R}_+ \times \mathbb{R}^{2n}, \mathbb{R}_+]$ *and* $V(t, \mathbf{x})$ *is locally Lipschitzian in* $\mathbf{x}$;
3) *for* $(t, \mathbf{x}) \in \mathbb{R}_+ \times S(A)$, $b_1(\|\mathbf{x} - \mathbf{x}^*\|) \leq V(t, \mathbf{x}) \leq b_2(\|\mathbf{x} - \mathbf{x}^*\|)$, $b_1, b_2 \in K$ *and* $D^+ V(t, \mathbf{x}) \leq q(t, V(t, \mathbf{x}))$, $q \in C[\mathbb{R}_+^2, \mathbb{R}]$;
4) $b_2(\lambda) < b_1(A)$ *holds.*

Then the practical stability properties of the scalar differential equation

$$z'(t) = q(t, z), \quad z(t_0) = z_0 \geq 0,$$

imply the corresponding practical stability properties of system (4).

III. Velocity Controllers

Our control objective is to construct the instantaneous velocity $(v_i(t), w_i(t))$, $t \geq 0$, for every individual $i \in \mathbb{N}$ via a Lyapunov-like function that satisfies Theorem 1. We will use the following two terms from [9] as we develop our Lyapunov-like function for system (4):

1) A *cohesive swarm* is a group (of individuals or agents) in which the distances between individuals are bounded from above.
2) A *well-spaced swarm* is a group (of individuals or agents) which does not collapse into a tight cluster.

Members of a cohesive group tend to stay together and avoid dispersing. In a well-spaced swarm, some minimal bin size exists such that each bin contains at most one individual. Moreover, the size of such a bin is independent of the number of individuals in the group.

A. Attraction to the Centroid

We can ensure that individuals are attracted to each other and also form a cohesive group by first having a measurement of the distance from the ith individual to the swarm centroid. This is the concept behind *flock centering*, which is one of the well-known three heuristic flocking rules of Reynolds' [18]. The rule minimizes the exposure of a member of a flock to the flock's exterior by having the member move toward the perceived center of the flock. It is therefore a form of attraction between individuals. Centering necessitates a measurement of the distance from the the ith individual to the swarm centroid. Thus, we consider the following function, for $i \in \mathbb{N}$,

$$R_i(\mathbf{x}) := \frac{1}{2} \left[\left(x_i - \frac{1}{n} \sum_{i=1}^{n} x_i \right)^2 + \left(y_i - \frac{1}{n} \sum_{i=1}^{n} y_i \right)^2 \right].$$

This will be part of a Lyapunov-like function for system (4), and as we shall see later, its role is to ensure that ith individual is attracted to the swarm centroid.

B. Inter-individual Collision Avoidance

The short-range repulsion between individuals necessitates first a measurement of the distance between the ith and the jth individuals, $j \neq i$, $i, j \in \mathbb{N}$. With equation (1) of the ith individual in mind, we consider the following function for this purpose:

$$Q_{ij}(\mathbf{x}) := \frac{1}{2} \left[(x_i - x_j)^2 + (y_i - y_j)^2 - (r_i + r_j)^2 \right].$$

This will also be part of the same Lyapunov-like function.

C. A Lyapunov-like Function and Well-Spaced Swarms

Let there be real numbers $\gamma_i > 0$, $\beta_{ij} > 0$ for $i, j = 1, \ldots, n$. Let

$$L_i(\mathbf{x}) := \gamma_i R_i(\mathbf{x}) + \sum_{\substack{j=1, \\ j \neq i}}^{n} \frac{\beta_{ij} R_i(\mathbf{x})}{Q_{ij}(\mathbf{x})}.$$

Consider as a tentative Lyapunov-like function for system (4),

$$L(\mathbf{x}) := \sum_{i=1}^{n} L_i(\mathbf{x}). \tag{5}$$

It is clear that L is continuous and locally positive definite over the domain

$$D(L) := \left\{ \mathbf{x} \in \mathbb{R}^{2n} : \sum_{i=1}^{n} \sum_{\substack{j=1, \\ j \neq i}}^{n} Q_{ij}(\mathbf{x}) > 0 \right\}.$$

Note that $L(\mathbf{x}^*) = 0$. However, $\mathbf{x}^* \notin D(L)$ since

$$\sum_{i=1}^{n} \sum_{\substack{j=1, \\ j \neq i}}^{n} Q_{ij}(\mathbf{x}^*) = -\frac{1}{2} \sum_{i=1}^{n} \sum_{\substack{j=1, \\ j \neq i}}^{n} (r_i + r_j)^2 < 0.$$

This is indeed a desirable situation since if $\mathbf{x}^* \in D(L)$, and if at some time $t \geq 0$, we have that $\mathbf{x} = \mathbf{x}^*$, then this implies that the swarm has collapsed onto itself, a biologically impossible

situation. As we alluded to earlier, we are not interested in the centroid, but in the behavior of our swarm in the vicinity of its centroid. In other words, we are interested in a well-spaced swarm.

The time-derivative of L along every solution of system (4) is the dot product of the gradient of L, given by,

$$\nabla L = \left(\frac{\partial L}{\partial x_1}, \frac{\partial L}{\partial y_1}, \cdots, \frac{\partial L}{\partial x_n}, \frac{\partial L}{\partial y_n} \right),$$

and the time-derivative of the state vector $\mathbf{x} = (x_1, y_1, \ldots, x_n, y_n)$. That is,

$$
\begin{aligned}
\dot{L}(\mathbf{x}) &= \nabla L(\mathbf{x}) \bullet \dot{\mathbf{x}} \\
&= \sum_{i=1}^{n} \left(\gamma_i \dot{R}_i(\mathbf{x}) + \sum_{\substack{j=1, \\ j \neq i}}^{n} \frac{\beta_{ij}}{Q_{ij}(\mathbf{x})} \dot{R}_i(\mathbf{x}) \right. \\
&\quad \left. - \sum_{\substack{j=1, \\ j \neq i}}^{n} \frac{\beta_{ij} R_i(\mathbf{x})}{Q_{ij}^2(\mathbf{x})} \dot{Q}_{ij}(\mathbf{x}) \right).
\end{aligned}
$$

Now, collecting terms with x_i' and y_i', and substituting $x_i' = \dot{x}_i = v_i$ and $y_i' = \dot{y}_i = w_i$ from system (3), we have

$$
\begin{aligned}
\dot{L}(\mathbf{x}) &= \sum_{i=1}^{n} \left[\frac{\partial L}{\partial x_i} \cdot \dot{x}_i + \frac{\partial L}{\partial y_i} \cdot \dot{y}_i \right] \\
&= \sum_{i=1}^{n} \left[\frac{\partial L}{\partial x_i} \cdot v_i + \frac{\partial L}{\partial y_i} \cdot w_i \right],
\end{aligned}
$$

where

$$
\begin{aligned}
\frac{\partial L}{\partial x_i} &= \left(\gamma_i + \sum_{\substack{j=1, \\ j \neq i}}^{n} \frac{\beta_{ij}}{Q_{ij}(\mathbf{x})} \right) \left(x_i - \frac{1}{n} \sum_{k=1}^{n} x_k \right) \\
&\quad - 2 \sum_{\substack{j=1, \\ j \neq i}}^{n} \frac{\beta_{ij} R_i(\mathbf{x})}{Q_{ij}^2(\mathbf{x})} (x_i - x_j), \tag{6}
\end{aligned}
$$

and

$$
\begin{aligned}
\frac{\partial L}{\partial y_i} &= \left(\gamma_i + \sum_{\substack{j=1, \\ j \neq i}}^{n} \frac{\beta_{ij}}{Q_{ij}(\mathbf{x})} \right) \left(y_i - \frac{1}{n} \sum_{k=1}^{n} y_k \right) \\
&\quad - 2 \sum_{\substack{j=1, \\ j \neq i}}^{n} \frac{\beta_{ij} R_i(\mathbf{x})}{Q_{ij}^2(\mathbf{x})} (y_i - y_j). \tag{7}
\end{aligned}
$$

Let there be real numbers $\mu_i > 0$ and $\varphi_i > 0$ such that

$$v_i = -\mu_i \frac{\partial L}{\partial x_i}, \quad \text{and} \quad w_i = -\varphi_i \frac{\partial L}{\partial y_i}.$$

Then for all $\mathbf{x} \in D(L)$,

$$
\begin{aligned}
\dot{L}(\mathbf{x}) &= -\sum_{i=1}^{n} \left[\mu_i \left(\frac{\partial L}{\partial x_i} \right)^2 + \varphi_i \left(\frac{\partial L}{\partial y_i} \right)^2 \right] \\
&= -\sum_{i=1}^{n} \left[\frac{v_i^2}{\mu_i} + \frac{w_i^2}{\varphi_i} \right] \leq 0.
\end{aligned}
$$

For the ith individual, system (3) therefore becomes

$$\left.\begin{array}{rcl} x_i'(t) & = & -\mu_i \dfrac{\partial L}{\partial x_i}, \ \ y_i'(t) = -\varphi_i \dfrac{\partial L}{\partial y_i}, \\[2mm] x_{i0} & = & x_i(t_0), \ \ y_{i0} = y_i(t_0), \ \ t_0 \geq 0. \end{array}\right\} \quad (8)$$

Define the $n \times n$ diagonal matrix

$$H = \mathrm{diag}(\underbrace{\mu_1, \varphi_1, \ldots, \mu_n, \varphi_n}_{2n \text{ elements}}).$$

Then our system (4) becomes the gradient system

$$\dot{\mathbf{x}} = \mathbf{G}(\mathbf{x}) = -H\left(\nabla L(\mathbf{x})\right), \ \mathbf{x}_0 := \mathbf{x}(t_0), \ t_0 \geq 0, \quad (9)$$

the ith term of which is given by (8). It is clear that $\mathbf{G} \in C[D(L), \mathbb{R}^{2n}]$.

D. Practical Stability

Theorem 2: System (9) is uniformly practically stable.
Proof: Since $\dot{L}(\mathbf{x}(t)) \leq 0$, we have

$$0 \leq L(\mathbf{x}(t)) \leq L(\mathbf{x}(t_0)) \ \ \forall \ t \geq t_0 \geq 0. \quad (10)$$

Accordingly, for comparative analysis, it is sufficient to consider the practical stability of the scalar differential equation

$$z'(t) = 0, \ \ z(t_0) =: z_0, \ \ t_0 \geq 0. \quad (11)$$

The solution is $z(t; t_0, z_0) = z_0$, so that relative to every point $z^* \in \mathbb{R}$, we have

$$z(t; t_0, z_0 - z^*) = z_0 - z^*,$$

and for any given number $P_0 > 0$, we have

$$|z(t; t_0, z_0 - z^*)| \leq |z_0 - z^*| + P_0.$$

We shall next show that whilst applying Theorem 1, we can simultaneously derive the explicit form of $P_0 > 0$, with which it is easy to see that (PS2) holds for equation (11) if

$$A = A(\lambda) := \lambda + P_0.$$

To apply Theorem 1, we restrict our domain to $D(L)$ over which we see that $L \in C[D(L), \mathbb{R}_+]$, and note that L is locally Lipschitzian in $D(L)$ since $dL/dt \leq 0$ in $D(L)$. Re-defining $S(\rho)$ as $S(\rho) = \{\mathbf{x} \in D(L) : \|\mathbf{x} - \mathbf{x}^*\| < \rho\}$, we get $S(A) = \{\mathbf{x} \in D(L) : \|\mathbf{x} - \mathbf{x}^*\| < \lambda + P_0\}$. Recalling that $\gamma_i > 0$, $i \in \mathbb{N}$, we let $\gamma_{\min} := \min_{i \in \mathbb{N}} \gamma_i$ and $\gamma_{\max} := \max_{i \in \mathbb{N}} \gamma_i$. Further, let

$$b_1(\|\mathbf{x} - \mathbf{x}^*\|) := \frac{1}{2}\gamma_{\min}\|\mathbf{x} - \mathbf{x}^*\|^2,$$

and

$$b_2(\|\mathbf{x} - \mathbf{x}^*\|) := \frac{1}{2}\gamma_{\max}\left[\|\mathbf{x} - \mathbf{x}^*\| + L(\mathbf{x}_0)\right]^2,$$

noting that $b_1, b_2 \in K$. Then assuming $P_0 > 0$ is given, we easily see that, with (10), we have, $b_1(\|\mathbf{x} - \mathbf{x}^*\|) \leq L(\mathbf{x}) \leq b_2(\|\mathbf{x} - \mathbf{x}^*\|)$ for all $\mathbf{x} \in S(A)$, since

$$\sum_{i=1}^{n} R_i(\mathbf{x}) = \frac{1}{2}\|\mathbf{x} - \mathbf{x}^*\|^2.$$

Indeed, the inequality $b_2(\lambda) < b_1(A)$ yields

$$\frac{1}{2}\gamma_{\max}\left[\lambda + L(\mathbf{x}_0)\right]^2 < \frac{1}{2}\gamma_{\min}[\lambda + P_0]^2,$$

which holds if we choose

$$P_0 > \left[\left(\sqrt{\frac{\gamma_{\max}}{\gamma_{\min}}} - 1\right) + \sqrt{\frac{\gamma_{\max}}{\gamma_{\min}}}L(\mathbf{x}_0)\right].$$

Since $\gamma_{\max}/\gamma_{\min} \geq 1$ for any $\gamma_{\max}, \gamma_{\min} > 0$, and because of (10), it is clear that P_0 exists and $P_0 > 0$. Thus, with $q(t, z) \equiv 0$, we conclude the proof of Theorem 2.

E. Insight into the form of the Lyapunov-like Function and Cohesiveness

Let us now discuss the idea behind the construction of our Lyapunov-like function $L(\mathbf{x})$. At large distances between the ith and the jth individuals, the ratio,

$$\sum_{i=1}^{n} \sum_{\substack{j=1, \\ j \neq i}}^{n} \frac{\beta_{ij} R_i(\mathbf{x})}{Q_{ij}(\mathbf{x})}, \quad (12)$$

is negligible, and the term $\sum_{i=1}^{n} \gamma_i R_i(\mathbf{x})$ dominates. Then, since $L(\mathbf{x}) \to 0$ as $\mathbf{x} \to \mathbf{x}^*$, the long-range attraction requirement in a swarm model is met, and $\sum_{i=1}^{n} \gamma_i R_i$ acts as the *attraction function*; each individual is attracted to the centroid, and therefore the swarm system (9) maintains centering and hence cohesiveness at all times. In fact, Theorem 2 proves the cohesiveness of the swarm, with the boundedness of solution for all time $t \geq t_0$ implying that distances between individuals are bounded from above at all times. Note that the parameter $\gamma_i > 0$ can be considered as a measurement of the strength of attraction between an individual i and the swarm centroid, and hence between each other. The smaller the parameter is, the weaker the cohesion of the swarm is. Hence, γ_i can be considered a *cohesion parameter*.

Consider now the situation where any two individuals i and j approach each other. In this case, Q_{ij} decreases and ratio (12) increases, with $\beta_{ij} > 0$ acting as a *coupling parameter* that is a measurement of the strength of interaction between the individuals. In this way, ratio (12) acts as an *inter-individual collision-avoidance function*, because it can be allowed to increase in value (corresponding to avoidance) as individuals approach each other. However, this increase cannot be unbounded in $D(L)$ because Theorem 2 shows that every solution $\mathbf{x}(t)$ of system (9) is bounded. In other words, collision-avoidance occurs without the danger of the individuals getting too close to each other, or the swarm collapsing on itself; simply $Q_{ij} = 0$ is not possible in $D(L)$. We have therefore met the short-range repulsion requirement in an individual-based model. Note that the increase in the ratio does not translate to an increase in $L \equiv L(t)$, simply because L is non-increasing in t and any increase in the ratio gives a smaller or the same value of L at time t compared to all previous values of L.

The choices of $\beta_{ij} > 0$ determine whether our system is *isotropic* (there is uniformity in attraction or repulsion between

all members of the swarm) or *anisotropic* (there are unequal attractive and repulsive forces). If $\beta_{ij} > 0$ are the same for all individuals, then we have an isotropic swarm model. If they differ between at least two individuals, then the model is anisotropic.

Finally, note that we have used two other parameters, $\mu_i > 0$ and $\varphi_i > 0$ in system (9). Because the parameters are a measure of the rate of decrease of $L \equiv L(t)$ at time $t \geq 0$, we name them *convergence parameters*. The larger the convergence parameters, the quicker the movements of the individuals toward and about the centroid.

F. Constant Arrangement About the Centroid

The Lyapunov-like function and Lasalle's invariance principle can be used to show that the swarm members can converge to a constant arrangement about a stationary centroid. This necessitates the inclusion of $\mathbf{x}^*$ in a domain over which system (9) remains continuous but is strictly Lyapunov stable.

Let

$$\mathcal{D} := \left\{ \mathbf{x} \in \mathbb{R}^{2n} : \sum_{i=1}^{n} \sum_{\substack{j=1, \\ j \neq i}}^{n} \frac{\beta_{ij} R_i(\mathbf{x})}{Q_{ij}(\mathbf{x})} \geq 0 \right\}.$$

Then since

$$\sum_{i=1}^{n} \sum_{\substack{j=1, \\ j \neq i}}^{n} \frac{1}{Q_{ij}(\mathbf{x}^*)} = -\sum_{i=1}^{n} \sum_{\substack{j=1, \\ j \neq i}}^{n} \frac{2}{(r_i + r_j)^2} \neq 0,$$

we have

$$\sum_{i=1}^{n} \sum_{\substack{j=1, \\ j \neq i}}^{n} \frac{\beta_{ij} R_i(\mathbf{x}^*)}{Q_{ij}(\mathbf{x}^*)} = 0.$$

This shows that $\mathbf{x}^* \in \mathcal{D}$. Moreover,

$$\frac{\partial L}{\partial x_i}(\mathbf{x}^*) = \frac{\partial L}{\partial y_i}(\mathbf{x}^*) = 0 \ \forall \ i \in \mathbb{N}, \tag{13}$$

with $L(\mathbf{x}) > 0$ for all $\mathbf{x} \in \mathcal{D} \setminus \mathbf{x}^*$, $L(\mathbf{x}^*) = 0$, and $\dot{L}(\mathbf{x}) \leq 0$ for all $\mathbf{x} \in \mathcal{D}$. Thus, we have found another set, given by $\mathcal{D} \supset D(L)$, over which the function $\mathbf{G}$ in (9) is continuous. That is, $\mathbf{G} \in C[\mathcal{D}, \mathbb{R}^{2n}]$, for which $L \in C^1[\mathcal{D}, \mathbb{R}_+]$ establishes stability in the Lyapunov sense. Now, $\partial L/\partial x_i$ and $\partial L/\partial y_i$, given in (6) and (7), respectively, are simply made up of polynomials and rational functions in x_i and y_i, with only Q_{ij} appearing in the denominator, and are continuous in $\mathcal{D}$. Similarly, $\partial^2 L/\partial x_i^2$ and $\partial^2 L/\partial y_i^2$ are made up of polynomials, if not constants, and rational functions in x_i and y_i, with only Q_{ij} appearing in the denominator, and are continuous in $\mathcal{D}$. Thus, $\mathbf{G} \in C^1[\mathcal{D}, \mathbb{R}^{2n}]$. This implies that $\mathbf{G}$ is locally Lipschitz on $\mathcal{D}$. Accordingly, letting $L_0 := L(\mathbf{x}(t_0))$, $t_0 \geq 0$, we have that the set

$$\Omega_{L_0} := \{\mathbf{x} \in \mathcal{D} : L(\mathbf{x}) \leq L_0\}$$

is a positively invariant set with respect to system (9). It is also compact because system (9) is Lyapunov stable, which implies the boundedness of solutions over $\mathcal{D}$. Let

$$E_1 := \{\mathbf{x} \in \Omega_{L_0} : \dot{L}(\mathbf{x}) = 0\}.$$

Then by LaSalle's invariance principle, every solution starting in Ω_{L_0} converges to the largest invariant set contained in E_1. Now, the set of all equilibrium points of (9) is

$$E_2 := \{\mathbf{x} \in \mathcal{D} : \frac{\partial L}{\partial x_i}(\mathbf{x}) = \frac{\partial L}{\partial y_i}(\mathbf{x}) = 0, i = 1, \ldots, n\},$$

noting that $\mathbf{x}^* \in E_2$ by (13). Then it follows easily that $E_2 = E_1$ since

$$\dot{L}(\mathbf{x}) = -\sum_{i=1}^{n} \left\{ \mu_i \left[\frac{\partial L}{\partial x_i}(\mathbf{x}) \right]^2 + \varphi_i \left(\frac{\partial L}{\partial y_i}(\mathbf{x}) \right)^2 \right\} = 0$$

if and only if, for $\mathbf{x} \in \mathcal{D}$,

$$\frac{\partial L}{\partial x_i}(\mathbf{x}) = \frac{\partial L}{\partial y_i}(\mathbf{x}) = 0 \ \forall \ i \in \mathbb{N}.$$

Since each point in E_2 is an equilibrium, E_2 is an invariant set. Hence, $\mathbf{x}(t) \to E_2$ as $t \to \infty$.

G. Size and Density of the Swarm

Given that a member i of the swarm resides in a disk defined in (1), with radius $r_i > 0$, we can follow the argument by Gazi and Passino [19] to estimate the size and density of the swarm in a stable arrangement, but without using their assumption that the swarm members had to be squeezed cohesively as closely as possible in an area (a disk) of radius r, since Theorem 2 already provides this cohesiveness. Indeed, since Theorem 2 establishes the practical stability of system (9) in $D(L)$, there is no collision between members in $D(L)$. Accordingly, between two members i and j, we have $\|\mathbf{x}_i(t) - \mathbf{x}_j(t)\| > (r_i + r_j)$, $\mathbf{x}_i = (x_i, y_i)$, for all time $t \geq t_0 \geq 0$. Now, the safety areas are disjoint, so the total area occupied by the swarm is $\pi \sum_{i=1}^{n} r_i^2$. By Theorem 2, given (λ, A), with $0 < \lambda < A$, we have $\|\mathbf{x}(t_0) - \mathbf{x}^*\| < \lambda$ implies $\|\mathbf{x}(t) - \mathbf{x}^*\| < A$ for all $t \geq t_0 \geq 0$. In such a practical stability arrangement, where all the solutions of (9) are bounded above by $A > 0$, we can therefore find a disk of radius, say, $p = p(A)$, around the centroid (x_c, y_c) such that $\pi p^2(A) \geq \pi \sum_{i=1}^{n} r_i^2$. From this we get $p_{\min} := (\sum_{i=1}^{n} r_i^2)^{1/2}$, a lower bound on the radius of the smallest circle which can enclose all the individuals. It is clear that the swarm size will scale with the size of the individual.

If we define the density of the swarm as the number of individuals per unit area, and let it be ρ, then it is simple to see that ρ is upper bounded, with $\rho \leq n/(\pi \sum_{i=1}^{n} r_i^2)$. Hence, the swarm cannot become arbitrarily dense.

H. Swarming in the Presence of Fixed Obstacles

If a swarm encountered an obstacle in its path, how would it behave? Nature provides instances of the resultant behaviors – a flock of bird may split and then rejoin [18]; a swarm of zooplankton *Daphnia magna* may swirl about a marker [20], [21]; a bacterial swarm may increase their density in the presence of antibiotics [22]; a school of fish may swirl [23].

In this subsection, we aim to show that it is straightforward to extend our model (9) to include fixed obstacles. For the purpose of illustrating our method, we consider the simplest obstacle, namely, a disk, which is a convex obstacle.

Let there be $m \in \mathbb{N}$ fixed obstacles modeled by disks centered at (o_{k1}, o_{k2}), $k = 1, \cdots, m$, with radii $r_{ok} > 0$. That is, $o_k := \left\{ (z_1, z_2) \in \mathbb{R}^2 : (z_1 - o_{k1})^2 + (z_2 - o_{k2})^2 \leq r_{ok}^2 \right\}$. For the avoidance of these fixed obstacles, we consider a measurement of the distance between the ith individual and o_k:

$$W_{ik}(\mathbf{x}) := \frac{1}{2} \left[(x_i - o_{k1})^2 + (y_i - o_{k2})^2 - (r_i + r_{ok})^2 \right].$$

Given some parameter $\alpha_{ik} > 0$, $i, k, \in \mathbb{N}$, which we will be our new *obstacle avoidance parameter* for fixed obstacle avoidance, we define a new function,

$$V_i(\mathbf{x}) = L_i + \sum_{k=1}^{m} \frac{\omega_{ik} R_i(\mathbf{x})}{W_{ik}(\mathbf{x})},$$

so that our new Lyapunov-like function for system (4) now becomes

$$V(\mathbf{x}) := \sum_{i=1}^{n} V_i(\mathbf{x}_i),$$

which is clearly continuous and locally positive definite on the domain

$$D(V) \quad := \quad \left\{ \mathbf{x} \in \mathbb{R}^{2n} : \sum_{i=1}^{n} \sum_{\substack{j=1, \\ j \neq i}}^{n} Q_{ij}(\mathbf{x}) > 0 \text{ and} \right.$$
$$\left. \sum_{i=1}^{n} \sum_{k=1}^{m} W_{ik}(\mathbf{x}) > 0 \right\},$$

noting that $\mathbf{x}^* \notin E(V)$. Now, carrying out the same analysis as in subsection III-C, we easily get, along a trajectory of system (4),

$$\dot{V}(\mathbf{x}) \quad = \quad -\sum_{i=1}^{n} \left[\mu_i \left(\frac{\partial V}{\partial x_i} \right)^2 + \varphi_i \left(\frac{\partial V}{\partial y_i} \right)^2 \right]$$
$$= \quad -\sum_{i=1}^{n} \left[\frac{v_i^2}{\mu_i} + \frac{w_i^2}{\varphi_i} \right] \leq 0,$$

for all $\mathbf{x} \in D(V)$, in which we have used the same parameters $\mu_i > 0$ and $\varphi_i > 0$ to obtain new instantaneous velocities:

$$v_i := -\mu_i \frac{\partial V}{\partial x_i}, \quad \text{and} \quad w_i := -\varphi_i \frac{\partial V}{\partial y_i},$$

where

$$\frac{\partial V}{\partial x_i} = \frac{\partial L}{\partial x_i} - \sum_{k=1}^{m} \frac{\alpha_{ik} R_i(\mathbf{x})}{W_{ik}^2(\mathbf{x})} (x_i - o_{k1}), \quad (14)$$

and

$$\frac{\partial V}{\partial y_i} = \frac{\partial L}{\partial y_i} - \sum_{k=1}^{m} \frac{\alpha_{ik} R_i(\mathbf{x})}{W_{ik}^2(\mathbf{x})} (y_i - o_{k2}). \quad (15)$$

Then system (4) becomes the new gradient system

$$\dot{\mathbf{x}} = \mathbf{G}(\mathbf{x}) = -H\left(\nabla V(\mathbf{x})\right), \ \mathbf{x}_0 := \mathbf{x}(t_0), \ t_0 \geq 0, \quad (16)$$

It is clear that $\mathbf{G} \in C[E(V), \mathbb{R}^{2n}]$. Using the same method of analysis as in subsection III-D, we can show that system (16) is practically stable.

IV. COMPUTER SIMULATIONS

In our computer simulations, we used the RK4 method to numerically integrate systems (9) and (16) to confirm the emergent collective behavior of a sufficiently large number of individuals governed by the systems. The system parameters played the major role in inducing several emergent patterns that are constant arrangements about the centroid.

A. Constant Arrangement about Centroid

Our first example (Figure 1) shows a convergence to a constant arrangement about a stationary centroid, and the second (Figure 2) a constant arrangement about a non-stationary centroid. In our model, this emergent pattern can be obtained if the cohesion parameters ($\gamma_i > 0, i \in \mathbb{N}$) are the same for all i, the coupling parameters ($\beta_{ij} > 0$, $i, j \in \mathbb{N}$, $i \neq j$) are the same for all i and j, and the convergence parameters ($\mu_i > 0$ and $\varphi_i > 0$) are the same for all $i \in \mathbb{N}$.
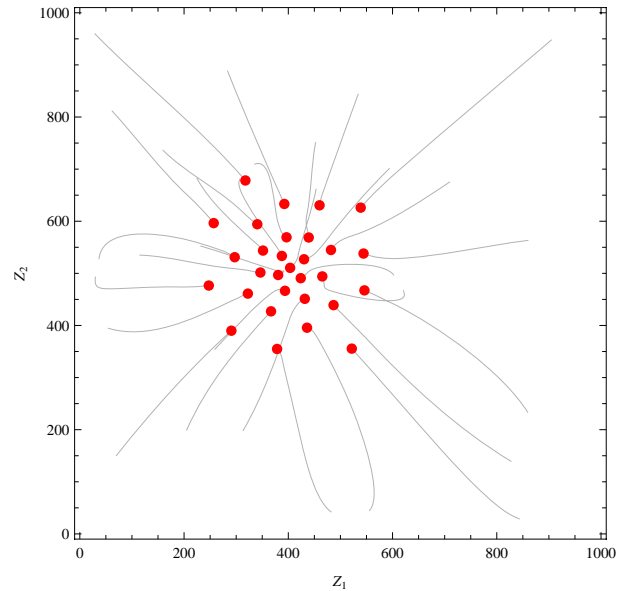

Fig. 1. **Example 1**: Convergence to a constant arrangement about a stationary centroid. Here, there are $n = 30$ individuals, each with bin size 10. The parameters, for all $i, j \in \mathbb{N}$, are $\gamma_i = 0.2$, $\beta_{ij} = 50$, and $\mu_i = \varphi_i = 0.1$. The individuals are randomly positioned initially. Their trajectories are shown in grey lines.

B. Swarming in the Presence of Obstacles

In this example, shown in Figure 3 ($n = 21$, and bin size is 8), individuals are attracted to each other from afar, avoid fixed obstacles ($m = 20$) and appear to meander initially between the obstacles before settling into a circular motion in a constant arrangement about the centroid.

V. APPLICATION TO PLANAR MOBILE UNICYLE-LIKE VEHICLES

In this section, we apply our method of developing the Lagrangian swarm model to design the velocity controllers of planar mobile unicycle-like robots. The ith vehicle's set of
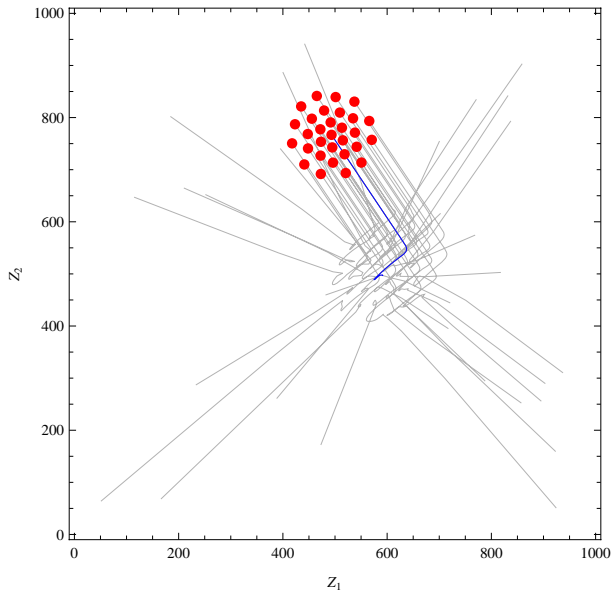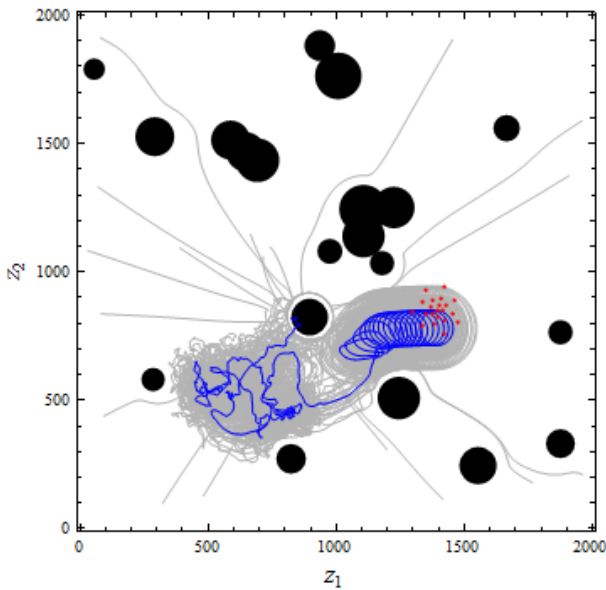
Fig. 2. Convergence to a constant arrangement about a non-stationary centroid whose path is shown by the thicker line. Here, there are $n = 30$ individuals, each with bin size 10. The parameters, for all $i, j \in \mathbb{N}$, are $\gamma_i = 2$, $\beta_{ij} = 50$, and $\mu_i = \varphi_i = 1$. The individuals were randomly positioned initially. Their trajectories are shown in grey lines.

Fig. 3. Whilst avoiding obstacles, the swarm eventually settles into a circular orbit. The thicker line traces the path of the centroid. The parameters, for all $i, j, k \in \mathbb{N}$, are $\gamma_i = 1$, $50 \leq \beta_{ij} \leq 200$ (randomized), $\omega_{ik} = 200$ and $\mu_i = \varphi_i = 1$. The individuals and fixed obstacles, with random sizes, were randomly positioned initially. Their trajectories are shown in grey lines.

kinematic equations, which involve the Cartesion position x_i, y_i, and its orientation angle, θ_i are [24]:

$$\left.\begin{array}{rcl} \dot{x}_i & = & v_i \cos \theta_i, \\ \dot{y}_i & = & v_i \sin \theta_i, \\ \dot{\theta}_i & = & \omega_i. \end{array}\right\} \quad (17)$$

We assume that the motion is governed by the combined action of both the angular velocity ω_i and the translational velocity v_i, and that v_i is in the direction of the one of axes of the vehicle. A negative v_i means that the ith vehicle is reversing along the opposite direction of the axis. A negative ω_i means that the ith vehicle is rotating clockwise.

In order to come up with some appropriate forms of the the velocities, let us, for the moment also assume the existence of a virtual length $\omega \geq 0$ originating from (x_i, y_i) and extending in the direction of v_i (see Figure 4). Then we we can consider a more general system, which we recognize as a simple car-like model:

$$\left.\begin{array}{rcl} \dot{x}_i & = & v_i \cos \theta_i - \xi \omega_i \sin \theta_i, \\ \dot{y}_i & = & v_i \sin \theta_i + \xi \omega_i \cos \theta_i, \\ \dot{\theta}_i & = & \omega_i. \end{array}\right\} \quad (18)$$

We will analyze this general system with the aim to obtain v_i and ω_i such that they do not depend on ξ. Then in such a case, we can let $\xi = 0$ to get back the original system (17).

To ensure that the ith vehicle safely steers pass other vehicles, we enclose it by a circle. By doing this, we are essentially following a well-known technique in mobile robot path-planning schemes wherein the robot is represented as a simpler fixed-shaped object, such as a circle, a polygon or a convex hull [25]. In our case, we can indeed take equation (1) as the definition of our car-like robots. Accordingly, our system consists of the robots B_i as members of a swarm, with $r_i = r$ for all $i \in \mathbb{N}$. The centroid of the swarm is given by (2). Our objective is to design the translational velocities v_i and the angular velocities ω_i such that robots are attracted to the centroid as a cohesive and well-spaced swarm.
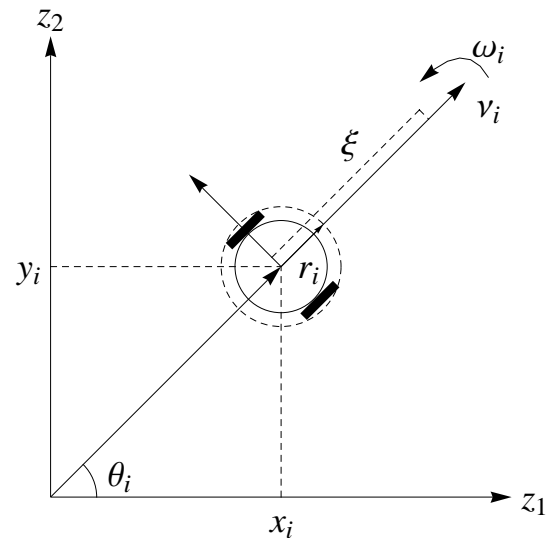

Fig. 4. The ith planar mobile unicycle-like vehicle.

A. Velocity Controllers for the Vehicles

Let us extend the definition of the independent variable from $\mathbf{x}_i = (x_i, y_i) \in \mathbb{R}^2$ to $\mathbf{x}_i = (x_i, y_i, \theta_i) \in \mathbb{R}^3$. Furthermore, with $\mathbf{x} := (\mathbf{x}_1, \ldots, \mathbf{x}_n) \in \mathbb{R}^{3n}$, we can use R_i for the

attraction to the centroid and Q_{ij} for inter-individual collision avoidance. Then applying the Lyapunov-like function (5) to system (18) over the domain

$$D(L) = \left\{ \mathbf{x} \in \mathbb{R}^{3n} : \sum_{i=1}^{n} \sum_{\substack{j=1, \\ j \neq i}}^{n} Q_{ij}(\mathbf{x}) > 0 \right\},$$

we have, noting that $\partial L/\partial \theta_i = 0$ since L does not contain a function of θ_i,

$$
\begin{aligned}
\dot{L}(\mathbf{x}) &= \sum_{i=1}^{n} \left[\frac{\partial L}{\partial x_i} x_i' + \frac{\partial L}{\partial y_i} y_i' \right] \\
&= \sum_{i=1}^{n} \left[\frac{\partial L}{\partial x_i} \left(v_i \cos \theta_i - \xi \omega_i \sin \theta_i \right) \right. \\
&\quad \left. + \frac{\partial L}{\partial y_i} \left(v_i \sin \theta_i + \xi \omega_i \cos \theta_i \right) \right] \\
&= \sum_{i=1}^{n} \left[\left(\frac{\partial L}{\partial x_i} \cos \theta_i + \frac{\partial L}{\partial y_i} \sin \theta_i \right) v_i \right. \\
&\quad \left. -\xi \left(\frac{\partial L}{\partial x_i} \sin \theta_i - \frac{\partial L}{\partial y_i} \cos \theta_i \right) \omega_i \right].
\end{aligned}
$$

Accordingly, we can define the control laws as

$$v_i := -K_i(\mathbf{x}) \left(\frac{\partial L}{\partial x_i} \cos \theta_i + \frac{\partial L}{\partial y_i} \sin \theta_i \right), \qquad (19)$$

and

$$\omega_i := M_i(\mathbf{x}) \left(\frac{\partial L}{\partial x_i} \sin \theta_i - \frac{\partial L}{\partial y_i} \cos \theta_i \right), \qquad (20)$$

where we want K_i and M_i to be some arbitrary positive functions continuous over $D(L)$ with the purpose to limit the size of the velocities, and $\partial L/\partial x_i$ and $\partial L/\partial y_i$ are as defined in (6) and (7), respectively. With these control laws, we have, with respect to system (18),

$$
\begin{aligned}
\dot{L}(\mathbf{x}) = & -\sum_{i=1}^{n} \left[K_i(\mathbf{x}) \left(\frac{\partial L}{\partial x_i} \cos \theta_i + \frac{\partial L}{\partial y_i} \sin \theta_i \right)^2 \right. \\
& \left. + \xi M_i(\mathbf{x}) \left(\frac{\partial L}{\partial x_i} \sin \theta_i - \frac{\partial L}{\partial y_i} \cos \theta_i \right)^2 \right] \leq 0.
\end{aligned}
$$

Following the proof of Theorem 2, which relies only on establishing that $\dot{L}(\mathbf{x}) \leq 0$, we can therefore infer the practical stability of the subsystem of system (18) made up of the first two terms (that is, $\dot{x}_i$ and $\dot{y}_i$). Hence, the vehicles, defined by their positions (x_i, y_i), are cohesive about their centroid. Their orientations are provided by the third term $\dot{\theta}_i$.

To find an explicit forms of $K_i > 0$ and $M_i > 0$, we note that

$$|v_i| \leq K_i \left(\left| \frac{\partial L}{\partial x_i} \right| + \left| \frac{\partial L}{\partial y_i} \right| \right)$$

and

$$|\omega_i| \leq M_i \left(\left| \frac{\partial L}{\partial x_i} \right| + \left| \frac{\partial L}{\partial y_i} \right| \right).$$

Since the maximum translational velocities and the maximum rotational velocities are

$$v_{\max} := \max_{i \in \mathbb{N}} |v_i| \quad \text{and} \quad \omega_{\max} := \max_{i \in \mathbb{N}} |\omega_i|,$$

we can easily get some appropriate forms of K_i and M_i. For example, if $\psi_1 > 0$ and $\psi_2 > 0$ are constants, then

$$K_i := \frac{v_{\max}}{\psi_1 + |\partial L/\partial x_i| + |\partial L/\partial y_i|}, \qquad (21)$$

and

$$M_i := \frac{\omega_{\max}}{\psi_2 + |\partial L/\partial x_i| + |\partial L/\partial y_i|}. \qquad (22)$$

These yield $|v_i| \leq v_{\max}$ and $|\omega_i| \leq \omega_{\max}$, respectively.

Finally, we let $\xi = 0$ in system (18). This has no effect on the controllers (19) and (20). Therefore, we get back our original system (17) with the same controllers.

Note that by simply replacing $\partial L/\partial x_i$ and $\partial L/\partial y_i$ by $\partial V/\partial x_i$ (equation (14)) and $\partial V/\partial y_i$ (equation (15)), respectively, in the controllers (19) and (20), we incorporate fixed obstacle avoidance capability.

B. Example 1: Swarming in the Absence of Fixed Obstacles

In this example, we show how multiple planar mobile unicycle-like robots swarm to eventually form a pattern in which their velocities and orientation stabilize.

There are 15 vehicles. Each vehicle is represented as an arrow, with the arrowhead showing the orientation θ_i, and direction of motion, and enclosed in a virtual protective circle of radius $r_i = 1.25$. The initial positions, orientations and velocities are randomized. The cohesion and coupling parameters are $\gamma_i = 1$ and $\beta_{ij} = 5$, $i, j \in \mathbb{N}$, respectively. The maximum translation and angular velocities are both 2. For the functions K_i shown in (21) and M_i in (22), we let $\psi_1 = \psi_2 = 1$.

We numerically integrate system (17) using the RK4 method to obtain Figures 5 to 8.
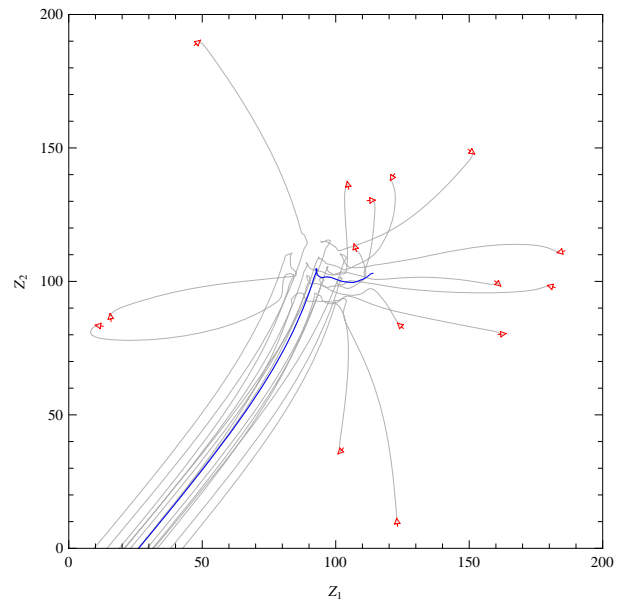

Fig. 5.   Example 1. The figure shows the initial orientations of the vehicles and their subsequent trajectories which are given in grey. The thicker trajectory is the trace of the centroid.
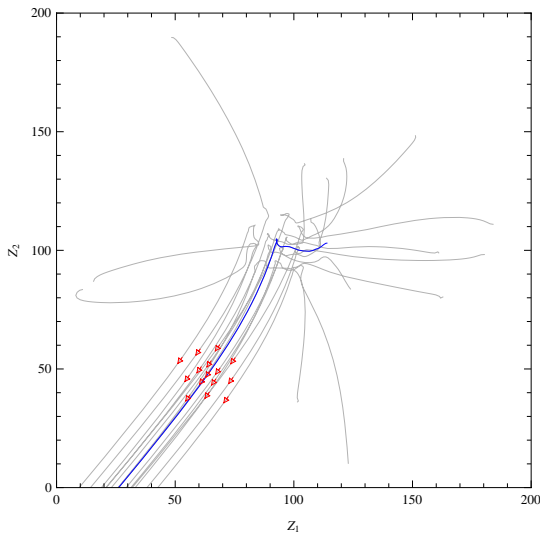
Fig. 6. By $t = 176$, the vehicles' velocities and orientation with respect to each other have already stabilized as depicted in Figures 7 and 8.
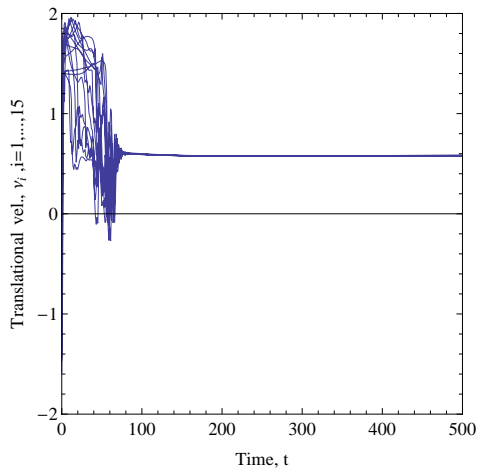

Fig. 7. Example 1. Stable translational velocities v_i of the vehicles. Recall that $v_{max} = 2$.

C. Example 2: Self-organized Oscillation

In this example with 5 vehicles, the vehicles eventually oscillate about a fixed point (Figure 9). The cohesion and coupling parameters are randomized with $0.1 \leq \gamma_i \leq 1$ and $5 \leq \beta_{ij} \leq 10$, $i, j \in \mathbb{N}$, respectively. The maximum translation and angular velocities are 1 and 2, respectively. For the functions K_i shown in (21) and M_i in (22), we let $\psi_1 = \psi_2 = 1$.

D. Example 3: Swarming in the Presence of Fixed Obstacles

In this example, the 15 vehicles considered in Example 1 now swarm in the presence of 10 fixed obstacles randomly placed and of random sizes. The controllers used are (19) and (20) but with $\partial L/\partial x_i$ and $\partial L/\partial y_i$, replaced by $\partial V/\partial x_i$ (equation (14)) and $\partial V/\partial y_i$ (equation (15)), respectively. The obstacle avoidance parameters are $\alpha_{ik} = 10$, $i, k \in \mathbb{N}$. As
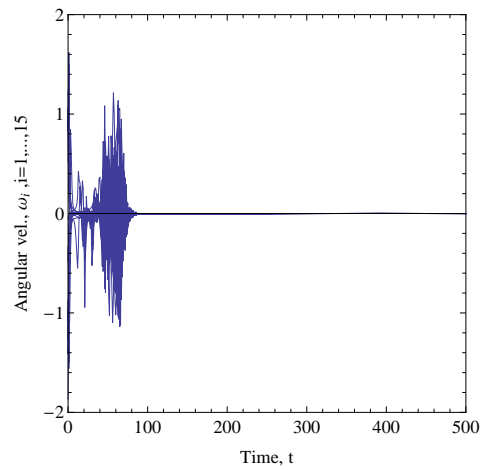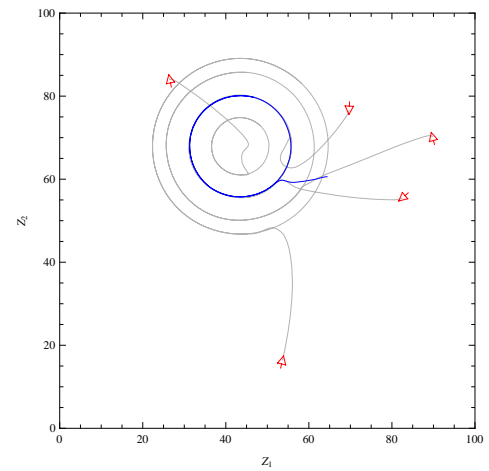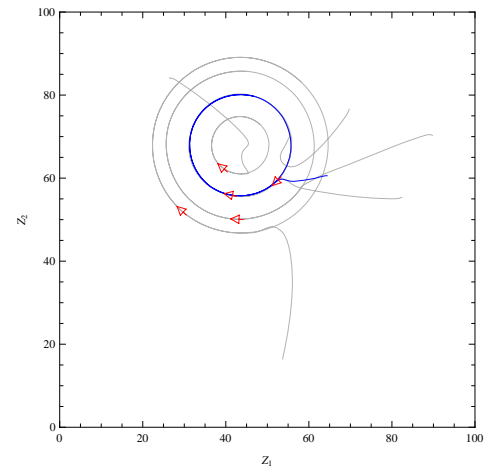

Fig. 8. Example 1. Stable angular velocities ω_i of the vehicles. Recall that $\omega_{max} = 2$.

(a)

(b)

Fig. 9. Example 2. Part (a) shows the initial positions and orientations of the vehicles. Part (b) shows that the emergent pattern is an oscillation about a fixed point.

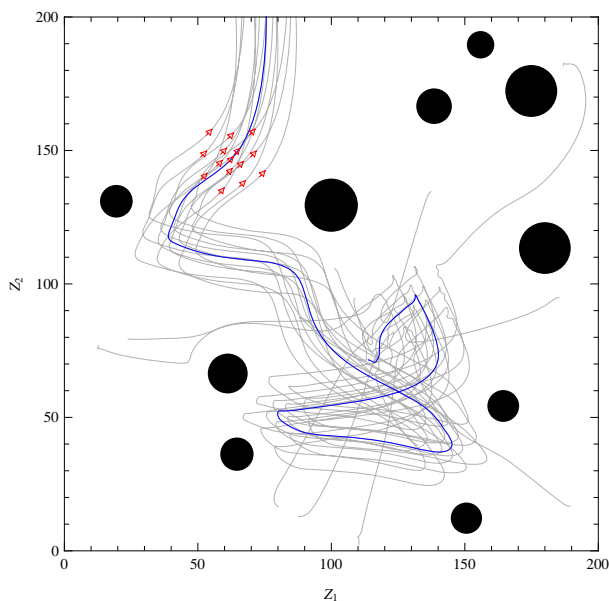shown in Figure 10, the vehicles successfully avoid these obstacles as a swarm.

Fig. 10.   Example 3. By $t = 730$, the swarm has begun the successful escape from the field of obstacles.

VI. Conclusion

Via a Lyapunov-like function, we developed a an attractive-repulsive swarm model and showed that it is a gradient system that is practically stable about the centroid. This implies that we could get a congregation of individuals about their centroid, forming cohesive and well-spaced swarms. Computer simulations illustrate this basic feature of collective behavior, with the associated parameters playing the major role in inducing the emergent collective behavior. Further, we showed how the basic model could be extended to include fixed obstacles. We then applied the methods expounded in this article to construct the velocity controllers of multiple planar unicycle-like robots such that they move in a coordinated fashion with respect to their centroid. The method is potentially applicable to the pattern formation and find-path problem of collaborating autonomous multi-agents.

References

[1] A. Okubo, *Diffusion and Ecological Problems: Mathematical Models*. Springer-Verlag NY, 1980.

[2] E. Bonebeau, M. Dorigo, and G. Theraulaz, *Swarm Intelliegence: From Natural to Artificial Systems*. New York: Oxford University Press, 1999.

[3] A. Martinoli, K. Easton, and W. Agassounon, "Modeling swarm robotic systems: A case study in collaborative distributed manipulation," *International Journal of Robotics Research*, vol. 23, no. 4, pp. 415–436, 2004, Special Issue on Experimental Robotics, P. Dario and B. Siciliano, editors. Invited paper.

[4] L. Edelstein-Keshet, "Mathematical models of swarming and social aggregation," in *Procs. 2001 International Symposium on Nonlinear Theory and Its Applications*, Miyagi, Japan, October-November 2001, pp. 1–7.

[5] E. Forgoston and I. B. Schwartz, "Delay-induced instabilities in self-propelling swarms," *Phys. Rev. E*, vol. 77, no. 3, p. 035203, Mar 2008.

[6] D. Grünbaum and A. Okubo, "Modelling social animal aggregations," in *Frontiers in Mathematical Biology. Lecture Notes in Biomathematics*, S. A. Levin, Ed. Springer-Verlag, Berlin, 1994, pp. 296–325.

[7] A. Mogilner and L. Edelstein-Keshet, "A non-local model for a swarm," *Journal of Mathematical Biology*, vol. 38, pp. 534–570, 1999.

[8] S. A. Levin, "Complex adaptive systems: Exploring the known, the unknown and the unknowable," *Bulletin of the Americal Mathematical Society*, vol. 40, no. 1, pp. 3–19, 2002.

[9] A. Mogilner, L. Edelstein-Keshet, L. Bent, and A. Spiros, "Mutual interactions, potentials, and individual distance in a social aggregation," *Journal of Mathematical Biology*, vol. 47, pp. 353–389, 2003.

[10] V. Gazi and K. Passino, "Stability analysis of social foraging swarms," *IEEE Transactions on Systems, Man and Cybernetics – Part B*, vol. 34, no. 1, pp. 539–557, 2004.

[11] A. J. Merrifield, "An investigation of mathematical models for animal group movement, using classical and statistical approaches," Ph.D. dissertation, University of Sydney, NSW, Australia, August 2006.

[12] V. Gazi and K. Passino, "Stability analysis of swarms," *IEEE Transactions on Automatic Control*, vol. 48, pp. 692–697, 2003.

[13] X.-B. Chen, F. Pan, L. Li, and H. Fang, "Practical stability analysis for swarm systems," in *IEEE Industrial Electronics, IECON 2006*, Paris, November 2006, pp. 3904–3909.

[14] F. Pan, X.-B. Chen, and L. Li, "Practical stability analysis of stochastic swarms," in *Innovative Computing Information and Control, 2008. ICICIC '08.*, Dalian, Liaoning, April 2008, p. 32.

[15] ——, "Practical stability in swarm systems," *Journal of Applied Mathematics and Informatics*, vol. 26, no. 1-2, pp. 203–212, 2008.

[16] Z. Xue and J. Zeng, "Practical stability analysis for exponential type stochastic swarms," in *International Conference on Computational Intelligence and Software Engineering*, Wuhan, 11-13 December 2009, pp. 1–4.

[17] V. Lakshmikantham, S. Leela, and A. A. Martynyuk, *Practical Stability of Nonlinear Systems*. Singapore: World Scientific, 1990.

[18] C. W. Reynolds, "Flocks, herds, and schools: A distributed behavioral model, in computer graphics," in *Proceedings of the 14th Annual Conference on Computer graphics and Interactive Techniques*, New York, USA, 1987, pp. 25–34.

[19] V. Gazi and K. Passino, "A class of attractions/repulsion functions for stable swarm aggregations," *International Journal of Control*, vol. 77, no. 18, pp. 1567–1579, 2004.

[20] A. Ordemann, G. Balazsi, and F. Moss, "Pattern formation and stochastic motion of the zooplankton *Daphina* in a light field," *Physica A*, vol. 325, pp. 260–266, 2003.

[21] F. Moss, "Into the *Daphina* vortex," *Chaos*, vol. 14, no. 4, p. S10, 2004.

[22] M. T. Butler, Q. Wang, and R. M. Harshy, "Cell density and mobility protect swarming bacteria against antibiotics," *Proceedings of the National Academy of Sciences*, vol. 107, no. 8, pp. 3776–3781, 2010.

[23] J. K. Parrish, S. Vicido, and D. Grümbaum, "Self-organized fish schools: An experimentation of emergent properties," *Biological Bulletin*, vol. 202, pp. 296–305, 2002.

[24] M. Aicardi, G. Casalino, A. Bicchi, and A. Balestrino, "Closed loop steering of unicycle-like vehicles via Lyapunov techniques," *IEEE Robotics and Automation Magazine*, vol. 2, no. 1, pp. 27–35, 1995.

[25] P. C.-Y. Sheu and Q. Xue, *Intelligent Robotic Planning Systems*. Singapore: World Scientific, 1993.